Theoretical Study of the Mechanism and Kinetics of Gas-Phase Ozone Additions to Ethene, Fluoroethene, and Chloroethene: A Multireference Approach

Ivan Ljubić* and Aleksandar Sabljić

Department of Physical Chemistry, Ruđer Bošković Institute, P.O. Box 180, HR-10002, Zagreb, Republic of Croatia

Ab initio multiconfigurational CASSCF and CASPT2 methods were employed in studying the reaction mechanisms and kinetics of the gas-phase ozone additions to ethene, fluoroethene, and chloroethene up to the formation of the primary addition products (primary ozonides). Reactants, transition-state structures, and products were optimized, and harmonic vibrational frequencies were calculated at the CASSCF/cc-pVTZ level. For kinetic calculations, the electron energies of all the stationary points were further refined by utilizing the CASPT2 method with the optimized CASSCF/cc-pVTZ wave functions taken as the zeroth order. The rate constants and Arrhenius kinetic parameters were finally calculated in terms of the conventional transition-state theory. The favorable conformations of the ozone approach to the two asymmetrically substituted haloalkenes are at first governed by the electrostatic repulsion in the transition-state structures and later by the gradually predominating anomeric effect. The bond formation in the primary haloozonides was analyzed by monitoring the changes in the occupation numbers of the active orbitals in the course of the optimizations. For all the reactions thus studied, close agreement is found with the experimental kinetics, which makes the future use of the same approach very promising.

Introduction

It is nowadays generally recognized that ozone represents one of the most important reactive species in the lower parts of the atmosphere.[1] For this reason, evaluation of the reactivity of alkenes and haloalkenes toward ozone is a substantial part of determining the half-life of these compounds in the atmosphere and, consequently, their impact on the global environment. It is highly desirable that all these compounds be depleted before they reach the upper parts, where they could participate in the destruction of the stratospheric ozone. Simple haloalkenes such as fluoro- and chloroethene are especially dangerous because of their widespread use as solvents and refrigerants. These are the pollutants of major concern, notably in industrial and urban areas. In organic synthesis, on the other hand, the ozonolytic reactions (ozonolyses) have long found their common application. Here, ozone is often used for cleaving carbon−carbon double bonds, whereby two carbonyl moieties result.[2]

Because ozonolyses of alkenes are reactions of great practical and theoretical interest, numerous experimental and theoretical studies have been carried out to elucidate their detailed kinetics and mechanistic aspects.[3] Special attention was paid to these reactions as a possible alternative source of OH radicals, the most important reactive species and the principal consumer in the lower parts of the atmosphere.[4] Although theoretical studies of the ozonolysis of the simplest alkene, ethene, conducted recently by Olzmann et al.[5] and Anglada et al.[6] seem to leave only a little space at present for further improvements and conclusions about this mechanism, very few theoretical studies have dealt with the ozonolyses of simple haloalkenes.[3d] Thus, to the best of our knowledge, no theoretical investigation of the ozonolysis of chloroethene has been carried out thus far.

The initial step of the ozonolysis of simple alkenes and haloalkenes is a thermally allowed [4 + 2] concerted electro-

**SCHEME 1: Initial Steps in the Ozonolysis of the (Halo)alkenes, (X = H, F, Cl)**
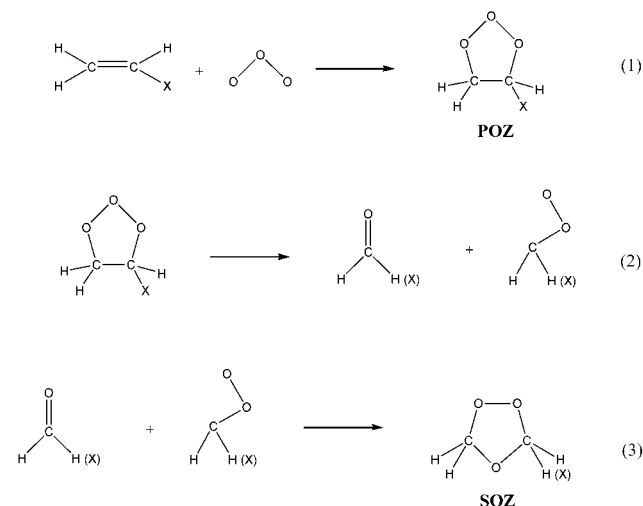
philic addition of ozone to the double bond of alkenes, producing 1,2,3-trioxolane, the primary ozonide **POZ**, in a highly stereo-specific manner (Scheme 1, step (1)). This step is very exo-thermic,[7] roughly by 50 kcal mol^{-1}, as was also theoretically confirmed.[3b,5,6] Hence, **POZ** is produced as a rather "hot" molecule vulnerable to further cleavage. The calculated height of the first potential barrier determines the Arrhenius parameters and the reaction rate constant, which can be directly compared to the experimental kinetics. Ethene-**POZ** was successfully isolated, and the puckering modes of its five-membered trioxo-lane ring were analyzed both experimentally and theoretically.[3c,d,8]

In the case of ethene, the electrophilic attack proceeds with C_s symmetry, with the favorable conformation along the reaction path governed mainly by the dipole−induced dipole interactions.[9] A single substitution by a halogen atom, on the other

* Corresponding author. E-mail: iljubic@rudjer.irb.hr.

hand, breaks any symmetry, which makes necessary a conformational analysis of the trend of the ozone approach with regard to the position of the halogen. Thus, the two pairs of transition structures and conformational minima of the monohalogenated **POZ**s exist with the apical O atom residing either on the side of (*syn*) or opposite to (*anti*) the halogen atom (Scheme 2.) These conformational minima are presumably separated by a low potential barrier for interchange of conformations.

SCHEME 2: *Syn* and *Anti* Conformations of the Primary (Halo)ozonides, (X = F, Cl)
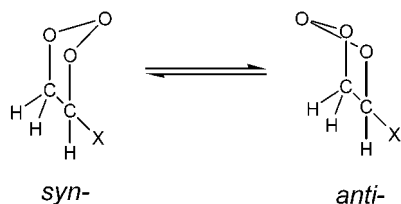
The reaction proceeds further by cleavage of **POZ**, which yields an aldehyde and a carbonyl oxide. The latter remarkable intermediate was named after Criegee, who was the first to postulate this sequence of ozonolytic reactions.[10] The possibilities of both mechanisms, stepwise and concerted, were proposed for this cleavage.[6] After that, the two products can rearrange in yet another electrophilic addition to form 1,2,4-trioxolane, the secondary ozonide (**SOZ**) (Scheme 1, steps 2 and 3). High stereoselectivity was observed in the course of the rearrangement to **SOZ**, the explanation of which was attempted in terms of the most favorable conformation for the cleavage to occur.[3b,c] The aldehyde−carbonyl oxide−vdW complex was proposed recently to account for the stereoselectivity effects in solutions.[3g,i] Again, in the case of monohalogenated primary addition products, two types of cleavage must be considered. As a result, the halogen atom is bonded either to the C atom of the carbonyl compound or to the Criegee intermediate.[1,11]

When choosing a correct theoretical method for describing an ozonolysis, one should bear in mind that the principal reactant, ozone, is a common example of a molecule in which near-degeneracy effects are very pronounced.[12] For this reason, ozone has long been considered to be an exceptionally demanding test case for quantum chemical methods. Nowadays, it is known that a high-quality description of the dynamical correlation and near-degeneracy effects is needed to obtain accurate enough geometry and a correct ordering of the vibrational frequencies. Nevertheless, in many studies, a reliable description of the ozone potential energy surface (PES) was attempted without employing any kind of multireference approach. The alternative to compensate for the near-degeneracy effects is to employ very elaborate post-HF methods,[13] whose use in studying reactions of ozone would obviously be prohibitively time consuming. As for the correlated multireference (MR) -based approaches, recently there have been increasingly efficient algorithms and well-formulated methods, some of which were also utilized in investigating the ozone PES.[14]

Logically, the general necessity for a multireference approach in describing ozone must also exist for any reaction involving it. Therefore, our aim in this work is to give a reliable and consistent theoretical description of the initial steps of the ozonolyses of ethene, fluoroethene, and chloroethene based entirely on the multiconfigurational CASSCF wave function and multireferent CASPT2 approach as formulated by Roos et al.[15] Although the CASPT2 method has proven to be particularly successful in studies of excited states and transition-metal complexes, its generally validity extends its area of application
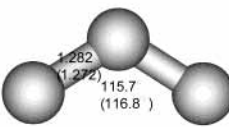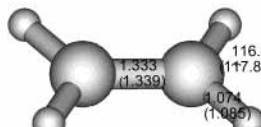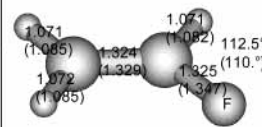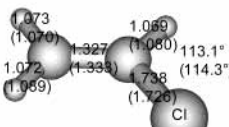
to any problem in electron structure theory.[16] Apart from its consistency of not mixing multiconfigurational optimizations with afterward single-referent energy refinements, applying the purely multiconfigurational computational approach provides us with the possibility of some great time savings. Once a satisfying zeroth-order wave function is obtained, which comprises all of the orbitals involved in the near-degeneracy effects, the CASPT2 approach with a large enough basis set turns out to be immensely cheaper than elaborate post-HF methods such as QCISD(T), CCSD(T), and MP4. Some of these were used in refs 5 and 6 to obtain acceptable energy differences for the first reaction barrier, which solely determines the kinetic parameters of ozonolysis. To achieve as much consistency as possible, our geometry optimizations and subsequent CASPT2 single-point calculations were carried out using the same large active space and basis set. Thus, the wave functions obtained in the course of the geometry optimizations that pertain to the stationary points on the PESs were used as the zeroth-order wave functions for CASPT2.

The reaction steps analyzed include the formation of the primary ozonides with discussion of the two basic distinct positions of the apical O atom in the case of the haloalkenes as well as the possibilities of the subsequent Criegee cleavages. The kinetic Arrhenius parameters and rate constants were then calculated in terms of the conventional transition-state theory[17] and compared to the experimental values.[1] Because the CASSCF method was conceived as a full configuration interaction (FCI) in a limited subspace of active orbitals, which are supposed to be chosen as the most important ones for the process of interest, we believe that valuable information can be extracted from analysis of the electronic structure in terms of these "best described" orbitals.

Theoretical Calculations

The geometries of reactants, transition states, and products were optimized, and harmonic vibrational frequencies were calculated at the CASSCF(10,9)/cc-pVTZ level of theory. This wave function is constructed of configurations made by all possible occupancies of 10 active electrons in the subspace of 9 active orbitals that when spin-adapted span the space of 5292 configuration state functions (CSFs). The same active-space size was used for all transition states and addition products and was chosen on the basis of the empirical prescription of Anglada and Bofill.[18] However, consistent active spaces for the independent reactants, which ensure a proper scaling of the energy, are determined by the choice made for the transition states. Hence, they must be (2,2) on the alkenes (π bonding and antibonding, 3 CSFs) and (8,7) on ozone (490 CSFs) without introducing any symmetry constraints. It must be noted that this way of partitioning the common active space between the independent reactants is different from the procedure described in ref 6. There, the optimal active spaces for all species were constructed from a diagonalized MRCI density matrix by including all the natural orbitals having occupancies between 0.02 and 1.98. Such a procedure led to a (2,2) active space on ethene and a (12,9) active space on ozone.[6] We further refined our CASSCF electron energies by accounting for the dynamical correlation via the CASPT2(10,9)/cc-pVTZ method using the wave functions from the optimized geometries as the zeroth order. The obtained geometries, vibrational frequencies, and electron energies corrected by the zero-point energies (ZPEs) were used in the calculations of the Arrhenius activation energies, preexponential factors, and reaction rate constants in terms of the conventional transition-state theory.[17] For all these

TABLE 1: Geometric Parameters (deg and Å) and Harmonic Vibrational Wavenumbers (cm^{-1})[a] for Reactants Ozone, Ethene, Fluoroethene, and Chloroethene Calculated at the CASSCF(8,7)/cc-pVTZ (Ozone) and CASSCF(2,2)/cc-PVTZ (All Remaining Reactants) Level of Theory[b]

modes	calc.	exp.	modes	calc.	exp.	modes	calc.	exp.	modes	calc.	exp.
σ	715	701	ρ(CH$_2$)	856	825	ρ(CH$_2$)	518	483	ρ(CH$_2$)	419	395
ν$_s$	1081	1103	Γ(CH$_2$)$_a$	883	943	Γ(CH$_2$)	683	711	Γ(CH$_2$)	589	620
ν$_a$	1243	1042	Γ(CH$_2$)$_s$	939	949	Γ(CH$_2$)	814	863	Γ(CH$_2$)	759	896
			τ(CH$_2$)	1088	995	ρ(CH$_2$)	944	929	ρ(CH$_2$)	863	720
			ρ(CH$_2$)	1335	1050	τ(CH$_2$)	1017	940	τ(CH$_2$)	968	941
			δ(CH$_2$)	1429	1342	ν(CF)	1270	1156	ν(CCl)	1124	1030
			δ(CH$_2$)	1586	1443	δ(CH$_2$)	1420	1306	δ(CH$_2$)	1394	1279
			ν(CC)	1752	1623	δ(CH$_2$)	1532	1380	δ(CH$_2$)	1501	1369
			ν(CH$_2$)$_s$	3268	2989	ν(CC)	1782	1654	ν(CC)	1726	1608
			ν(CH$_2$)$_s$	3285	3019	ν(CH$_2$)$_s$	3305	3080	ν(CH$_2$)$_s$	3294	3030
			ν(CH$_2$)$_a$	3340	3105	ν(CH)	3366	3115	ν(CH)	3369	3086
			ν(CH$_2$)$_a$	3370	3273	ν(CH$_2$)$_a$	3402	3150	ν(CH$_2$)$_a$	3390	3121

[a] ν-stretching, σ-scissoring, δ-bending, ρ-rocking, Γ-piramidal distortion, τ-torsion. [b] Experimental values are given in parentheses.

calculations, the basis set used was Dunning's polarized correlation consistent valence triple-ζ (cc-pVTZ), whose contractions are of the (4s3p2d1f) quality on O, C, and F atoms, (3s2p1d) on the H atom, and (5s4p2d1f) on the Cl atom.[19] Because of the inadequacy of this basis set to account for the core−valence and core−core correlation properly, core electrons were left uncorrelated in all cases (i.e., they were kept frozen). All electronic structure calculations were carried out with the program packages MOLCAS4.1[20] and MOLCAS5.0.[21] The POLYRATE package, version 7.8,[22] was utilized in the calculations involving reaction kinetics and thermodynamics. The calculations were done on IBM RISC/6000, DEC-Alpha500, and HP-kayak600 workstations.

Experimental Results

The kinetic studies of ozonolyses of many organic compounds and the corresponding reaction rates and Arrhenius parameters are collected and evaluated in the review by Atkinson and Carter.[1] Whereas the results for the ethene ozonolysis are really abundant,[23] quite the opposite can be said of the data involving fluoro- and chloroethene. Thus, only a single gas-phase study at two temperatures exists for fluoroethene,[23g] and three single-temperature gas-phase studies exist for chloroethene.[24] However, the discrepancy between the latter three is very large. It was noted that considerable difficulties and uncertainties in studies of gas-phase haloalkene ozonolyses are due to complicated secondary reactions; therefore, taking the obtained rate constants as upper limits was recommended. The following Arrhenius expression was obtained for ethene ozonolysis:[1]

$$k(\text{ethene}) = (1.20^{+0.31}_{-0.24}) \times$$
$$10^{-14} \exp[-(5232 \pm 117) \text{ cal}/RT] \text{ cm}^3 \text{ molecule}^{-1} \text{ s}^{-1}$$

The rate constant at 298 K is

$$k(\text{ethene, 298 K}) = (1.75 \pm 0.52) \times$$
$$10^{-18} \text{ cm}^3 \text{ molecule}^{-1} \text{ s}^{-1}$$

The following expression based on the single study can be deduced for fluoroethene:

$$k(\text{fluoroethene}) =$$
$$1.49 \times 10^{-13} \exp[-7200 \text{ cal}/RT] \text{ cm}^3 \text{ molecule}^{-1} \text{ s}^{-1}$$

The rate constant at 298 K is

$$k(\text{fluoroethene, 298 K}) = 7.81 \times 10^{-19} \text{ cm}^3 \text{ molecule}^{-1} \text{ s}^{-1}$$

with unknown uncertainties. No recommendation can be given for the rate constant of chloroethene ozonolysis. All available kinetic data together with the calculated values are displayed in Figures 7, 8, and 9 of the Reaction Kinetics section.

Results and Discussion

A. Optimized Structures and Vibrational Frequencies

1. Reactants. Geometric parameters of the fully optimized reactants and the calculated harmonic vibrational wavenumbers are given in Table 1. The geometric parameters of the alkenes are in somewhat poorer agreement with the experimental values[25] than those optimized at the MP2/6-311+G(2d,p) level,[26] especially concerning the length of the C−halogen bond, which is 0.022 Å shorter in fluoroethene and 0.012 Å longer in chloroethene. The reasons for this difference lie in the fact that CASSCF(2,2) is just a small step away from the simple HF, taking under explicit consideration only the π-electron density of C−C double bond. Thus, a closer approach of CASSCF to the experimental values and a better performance over HF is expected only in the case of the double C−C bond, whereas the C−halogen bond is stays approximately the same length. This is exactly what happens, for the sake of comparison, when HF/cc-pVTZ optimization of fluoroethene yields 1.306 Å (0.023 Å short of experiment!) for the double bond and 1.321 Å for the C−F bond. The correlation coefficients between experimental[27] and theoretical harmonic wavenumbers range from 0.996 for ethene to 0.999 for fluoroethene. The scaling factors of 0.9312, 0.9349, and 0.9270 minimize the squares of the

TABLE 2: Geometric Parameters (deg and Å) and Harmonic Vibrational Wavenumbers (cm^{-1}) for Transition State TS and Primary Addition Product POZ Formed in the Ozonolysis of Ethene Calculated at the CASSCF(10,9)/cc-pVTZ Level of Theory[a]

Vibrational wavenumbers/ cm^{-1}

i664, 149, 231, 429, 442, 663, 726, 876, 883, 1005, 1040, 1049, 1092, 1291, 1325, 1581, 1660, 3291, 3302, 3378, 3404

Vibrational wavenumbers/ cm^{-1}

147, 437, 765, 784, 887, 954, 994, 1008, 1129, 1155, 1214, 1274, 1289, 1420, 1421, 1583, 1598, 2987, 3002, 3263, 3278

[a] Experimental values obtained from the microwave spectra[8] are given in parentheses.

differences, and the largest deviations remain for $\rho(CH_2)_{ethene}$ (193 cm^{-1}), $\Gamma(CH_2)_{fluoroethene}$ (102 cm^{-1}), and $\Gamma(CH_2)_{chloroethene}$ (192 cm^{-1}). It can be seen that the substitution of fluorine on ethene leads to an increase in the C−C stretching frequency and a decrease in the torsion around the C−C bond, which indicates weakening of the π bond and strengthening of the σ bond in fluoroethene. In chloroethene, both of these frequencies are decreased. Experimentally determined ionization potentials[28] reveal that the fluoroethene HOMO is stabilized and the chloroethene HOMO is destabilized compared to those of ethene. All the net effects result from the resonant (π-donor) and inductive capabilities of the halogen atoms, and the consequent net distribution of charge has a decisive impact on the rates of fluoroethene and chloroethene ozonolysis.

The incorrect ordering of the calculated wavenumbers of ozone is a well-known occurrence involving methods that are deficient in their descriptions of either dynamical or nondynamical correlation. It was shown only recently[14d] that accurate and correctly ordered frequencies can be obtained by means of the reduced MR coupled cluster method with inclusion of all three possible spin-adapted references of the (2,2) active space, which unconstrains the symmetry adaptation. Because our CASSCF(8,7)/cc-pVTZ calculation includes only a small fraction of the dynamical correlation, it also incorrectly puts the asymmetric mode above the symmetric one, thus overestimating the experimental value[29] by 201 cm^{-1}. The increase in active space up to the full outer valence (12,9)[30] does not result in a convincing approach of the calculated geometric parameters toward the experimental values.[31] Still, the parameters are in a fairly good agreement with the experiment for the (8,7) ozone active space used throughout this work (Table 1).

2. Transition-State Structures. The geometric parameters and harmonic vibrational wavenumbers for the transition states and addition products for the ozonolyses of ethene, fluoroethene, and chloroethene are given in Tables 2, 3, and 4, respectively (**TS**, **TSF**, **TSCl**, **POZ**, **POZF**, and **POZCl**).

Hereafter, C bonded to any of the halogen atoms (X) and the terminal O attacking this C are labeled C2 and O3, respectively, and the remaining C and terminal O are labeled C1 and O2, respectively. The two conformations will be referred to as *syn* (apical O (O1) and halogen atoms on the same side of the C−C−O−O−O envelope, (X−C2−O3−O1) dihedral less than 90°) and *anti* (apical O and halogen atoms on different

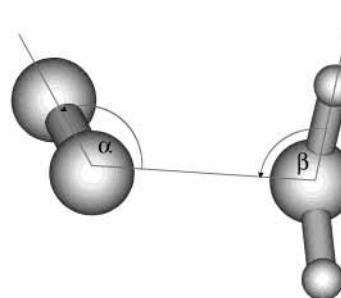**Figure 1.** Conformation of the transition state **TS** between ozone and ethene characterized by the two obtuse angles $\alpha = 125°$ and $\beta = 93°$ and designated *syn a* in ref 9. ($\alpha = 111°$ and $\beta = 107°$ in the prereaction vdW complex[9]).

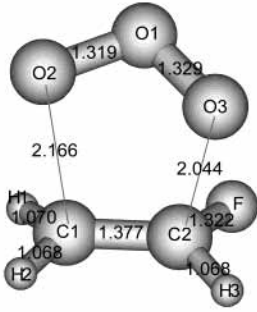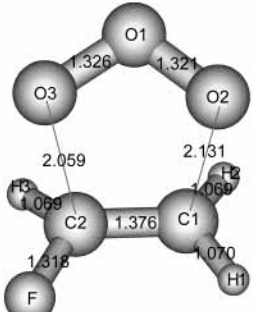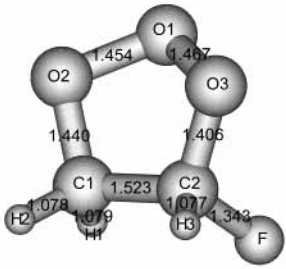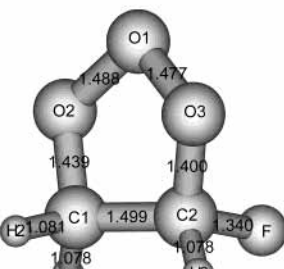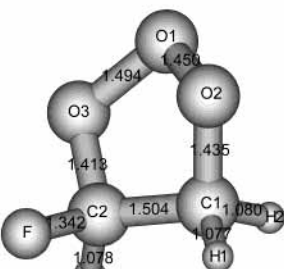sides of the C−C−O−O−O envelope, (X−C2−O3−O1) dihedral greater than 90°).

The analysis of the transition vectors in all transition states confirms that along these vectors the primary addition products (**POZ**s) are to be formed. All transition states can be characterized as a rather early type because they are much more reactant-like. For instance, the C−C bond is on average only 4% longer than in the independent (halo)alkenes. Hence, the Hammond postulate suggests a small reaction barrier and a highly exothermic reaction. Consequently, primary ozonides are formed as rather hot and under tropospheric conditions, unstable molecules.

TS possesses C_s symmetry with the most favorable conformation governed by the dipole−induced dipole interactions analogous to those in the prereaction vdW complex, as was put forward by C. W. Gillies et al.[9] This conformation is characterized by the angles α and β that are both obtuse as shown in Figure 1. The calculated bond distances can be compared to the other theoretical findings.[5,6] The largest differences between our values and those of CASSCF(10,9)/6-31G(d) is in the O−O−O angle (−6.2°), the O−O bond length (−0.011 Å), and the C−O distance (−0.012 Å). The B3LYP method is unsuccessful in the search for a reasonable geometry for **TS**.[6]

In the two pairs of ozone−haloalkene transition states (*syn*- and *anti*-**TSF**s and **TSCl**s), a geometrical trend different from that in **TS** is observed for the haloalkene moieties. Namely, whereas in **TS** the cis vicinal H atoms are perfectly eclipsed throughout the reaction path and the whole structure undergoes

Ozonolyses of Ethene and Fluoro- and Chloroethene

J. Phys. Chem. A, Vol. 106, No. 18, 2002 **4749**

TABLE 3: Geometric Parameters (deg and Å) and Harmonic Vibrational Wavenumbers (cm⁻¹) for Transition States TSFs and Primary Addition Products POZFs Formed in the Ozonolysis of Fluoroethene and Calculated at the CASSCF(10,9)/cc-pVTZ Level of Theory
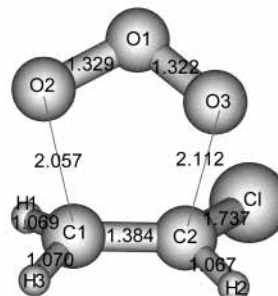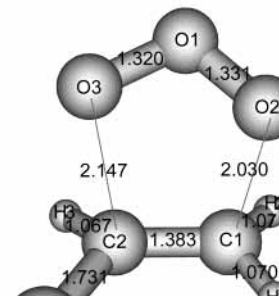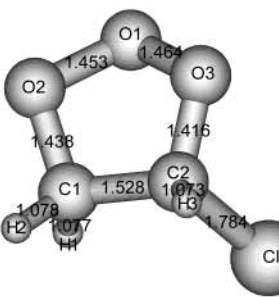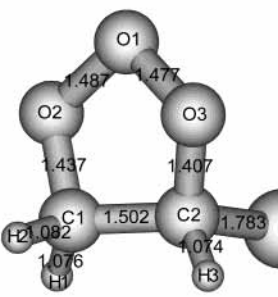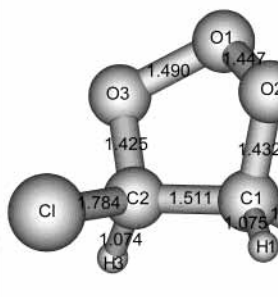

syn-TS ozone-fluoroethene

θ(O2-O1-O3)=108.3°
θ(H3-C2-F)=113.4°
δ(F-C2-O3-O1)=76.7°
δ(H2-C1-C2-H3)=11.3°

Vibrational wavenumbers/cm⁻¹

i736, 121, 193, 233, 419, 516, 583, 732, 775, 877, 963, 1008, 1042, 1084, 1274, 1329, 1516, 1633, 3318, 3385, 3428

anti-TS ozone-fluoroethene

θ(O2-O1-O3)=108.6°
θ(H3-C2-F)=113.2°
δ(F-C2-O3-O1)=142.9°
δ(H2-C1-C2-H3)=7.8°

Vibrational wavenumbers/cm⁻¹

i732, 122, 200, 279, 431, 481, 536, 718, 813, 879, 967, 1001, 1037, 1086, 1274, 1342, 1527, 1637, 3315, 3380, 3423

syn-primary fluorozonide

θ(O2-O1-O3)=100.6°
θ(C1-O2-O1)=101.0°
θ(C1-C2-O3)=105.1°
θ(C2-O3-O1)=102.3°
θ(H3-C2-F)=108.1°
δ(O2-C1-C2-O3)=−1.8°
δ(H2-C1-C2-H3)=−0.2°
δ(F-C2-O3-O1)=90.6°

Vibrational wavenumbers/cm⁻¹

114, 332, 457, 568, 691, 756, 809, 835, 946, 1040, 1100, 1165, 1229, 1330, 1451, 1466, 1527, 1623, 3233, 3284, 3301

TS between conformations

θ(O2-O1-O3)=106.1°
θ(C1-O2-O1)=105.3°
θ(C1-C2-O3)=103.7°
θ(C2-O3-O1)=104.6°
θ(H3-C2-F)=109.0°
δ(O2-C1-C2-O3)=40.2°
δ(H2-C1-C2-H3)=37.5°
δ(F-C2-O3-O1)=81.8°

Vibrational wavenumbers/cm⁻¹

i137, 189, 428, 524, 673, 754, 814, 890, 962, 1051, 1064, 1159, 1228, 1329, 1452, 1487, 1517, 1623, 3217, 3285, 3295

anti-primary fluorozonide

θ(O2-O1-O3)=104.1°
θ(C1-O2-O1)=100.5°
θ(C1-C2-O3)=105.0°
θ(C2-O3-O1)=105.7°
θ(H3-C2-F)=108.1°
δ(O2-C1-C2-O3)=35.5°
δ(H2-C1-C2-H3)=36.5°
δ(F-C2-O3-O1)=109.3°

Vibrational wavenumbers/cm⁻¹

106, 283, 460, 491, 665, 757, 825, 858, 967, 1032, 1042, 1150, 1237, 1337, 1443, 1480, 1528, 1610, 3224, 3279, 3308

an expected symmetry-consistent descent into **POZ**, in all **TSX**s, the H atoms are always staggered, sometimes considerably as in *syn*-**TSF** where δ(H2−C1−C2−H3) = 11°. Furthermore, such a torsion around the C−C bond is quite uneven as, for example, in *syn*-**TSF** where δ(H2−C1−C2−F) = 2°. An inspection of orbital coefficients of HOMOs and (HOMOs-1) in **TSX**s reveals that the haloalkene moieties are distorted in such a way as to retain a significant π overlap between the C atoms and the halogen, which suggests an importance of the prolonged stabilization in **TSX**s via the halogen π donor activity. It should be noted that the described torsion is an "unnecessary" move-

ment in *syn*-**TSF** in view of the corresponding geometry trend in *syn*-**POZF**, where the vicinal H atoms are once again eclipsed.

Interestingly enough, the transition states involving the two asymmetrically substituted alkenes are characterized by the different trends of the ozone approach. Namely, in **TSF**, the O3−C2 distance is substantially less than the O2−C1 distance, whereas in **TSCl**, the opposite is the case (Tables 3 and 4). The Mulliken population analysis, Figure 2, reveals that the charge excesses on the terminal O atoms are of a different trend as well. In **TSCl**, these charges are almost balanced, with O2

TABLE 4: Geometric Parameters (deg and Å) and Harmonic Vibrational Wavenumbers (cm⁻¹) for Transition States TSCls and Primary Addition Products POZCls Formed in the Ozonolysis of Chloroethene and Calculated at the CASSCF(10,9)/ cc-pVTZ Level of Theory

syn-TS ozone-chloroethene
θ(O2-O1-O3)=108.1°
θ(H2-C2-Cl)=113.8°
δ(Cl-C2-O3-O1)=80.8°
δ (H2-C2-C1-H3)=5.4°
Vibrational wavenumbers/cm⁻¹
i724, 105, 174, 218, 391, 478, 538, 730, 749, 797, 894, 985, 1044, 1082, 1143, 1304, 1436, 1618, 3316, 3397, 3420

anti-TS ozone-chloroethene
θ(O2-O1-O3)=108.4°
θ(H2-C2-Cl)=113.7°
δ(Cl-C2-O3-O1)=145.1°
δ(H2-C1-C2-H3)=2.0°
Vibrational wavenumbers/cm⁻¹
i713, 107, 161, 253, 389, 445, 502, 715, 774, 809, 883, 986, 1055, 1083, 1140, 1308, 1448, 1615, 3305, 3389, 3411

syn-primary chlorozonide
θ(O2-O1-O3)=100.6°
θ(C1-O2-O1)=100.4°
θ(C1-C2-O3)=105.0°
θ(C2-O3-O1)=102.9°
θ(H3-C2-Cl)=106.4°
δ(O2-C1-C2-O3)=-7.8°
δ(H2-C1-C2-H3)=-6.4°
δ(Cl-C2-O3-O1)=98.1°
Vibrational wavenumbers/cm⁻¹
87, 305, 363, 448, 660, 736, 774, 816, 834, 995, 1041, 1089, 1159, 1316, 1406, 1427, 1480, 1626, 3242, 3300, 3318

TS between conformations
θ(O2-O1-O3)=106.2°
θ(C1-O2-O1)=105.1°
θ(C1-C2-O3)=102.9°
θ(C2-O3-O1)=104.7°
θ(H3-C2-Cl)=107.4°
δ(O2-C1-C2-O3)=41.9°
δ(H2-C1-C2-H3)=39.0°
δ(Cl-C2-O3-O1) =83.5°
Vibrational wavenumbers/cm⁻¹
i107, 165, 355, 422, 659, 712, 751, 806, 880, 1010, 1022, 1103, 1164, 1304, 1402, 1418, 1481, 1623, 3208, 3305, 3315

anti-primary chlorozonide
θ(O2-O1-O3)=103.5°
θ(C1-O2-O1)=105.3°
θ(C1-C2-O3)=102.4°
θ(C2-O3-O1)=100.0°
θ(H3-C2-Cl)=106.6°
δ(O2-C1-C2-O3)=31.0°
δ(H2-C1-C2-H3)=33.0°
δ(Cl-C2-O3-O1)=118.3°
Vibrational wavenumbers/cm⁻¹
60, 274, 356, 419, 661, 739, 747, 818, 824, 993, 1016, 1093, 1167, 1319, 1404, 1423, 1479, 1614, 3219, 3303, 3319

being only slightly more negative. In **TSF**, on the other hand, O3 has a larger excess of negative charge, and the polarization between the terminal O atoms is much more pronounced. Meanwhile, the differences in charges on C atoms in transition structures are comparable to the ones found for independent haloalkenes.

Thus, significant polarization is preserved in the fluoroethene moiety because of the high electronegativity of the F atom. In this case, the inductive effects are predominant over the resonance π-donor ability of the F atom. In chloroethene, near-balance between the inductive effect and resonance activity of the Cl atom results in only a small excess of negative charge on both C atoms and therefore much weaker polarization of

the C—C bond. The main difference in charge on independent haloalkenes and on those in the transition states is found to be on C1. From here, some excess of negative charge (0.05−0.07 for *anti*-**TSF**−*syn*-**TSF** and 0.08−0.11 for *anti*-**TSCl**−*syn*-**TSCl**) is displaced on the ozone molecule and almost evenly distributed between the two terminal O atoms, whereas the apical O atom always gains somewhat more charge. Such a charge displacement formally confirms the electrophilic character of the ozone moiety. Although the overall occurrences weaken the polarization of the C—C double bond in **TSF**s as compared to that in the independent fluoroethene, the polarization is still strong enough for the substantial dipole−dipole interactions to govern the geometry trends in **TSF**. Hence, the scarcity of the
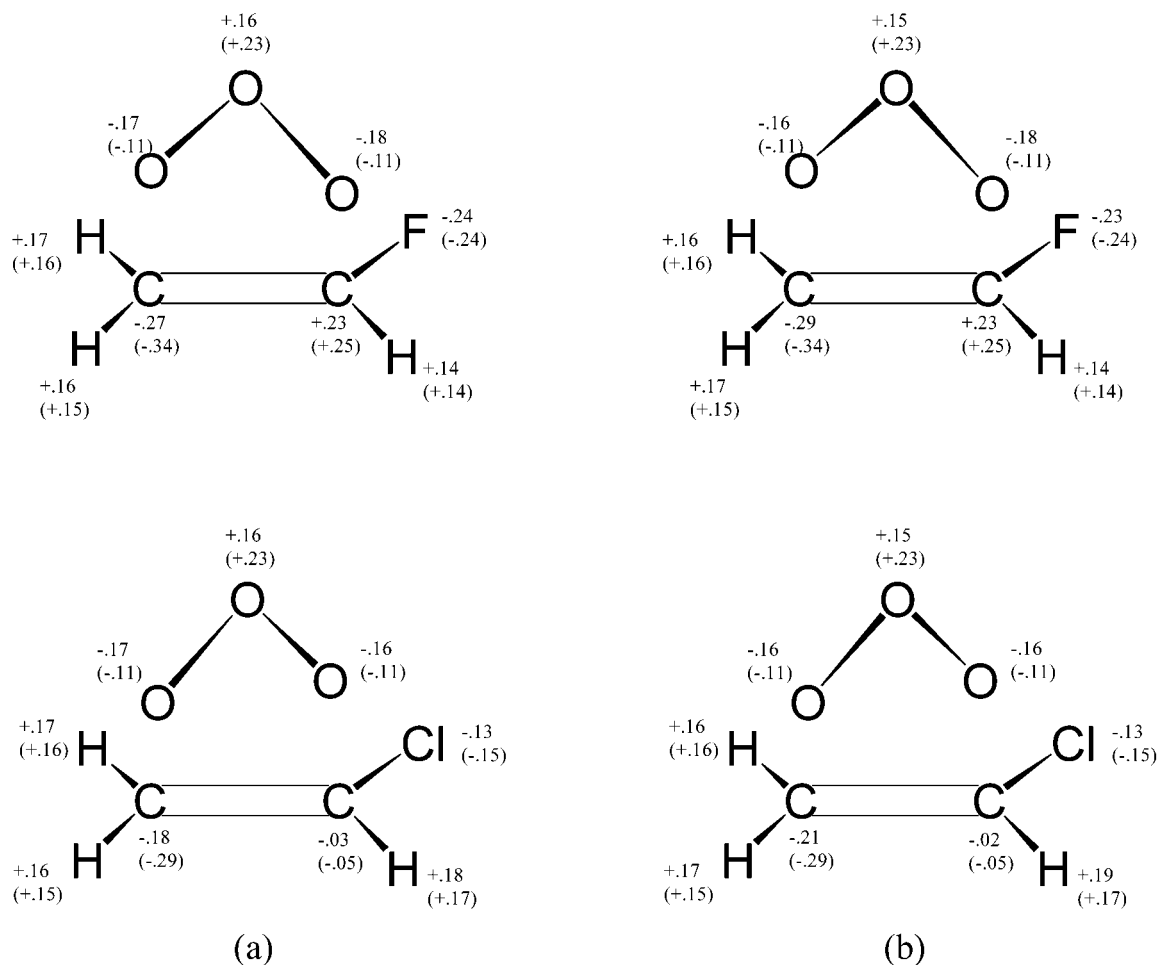
Ozonolyses of Ethene and Fluoro- and Chloroethene

J. Phys. Chem. A, Vol. 106, No. 18, 2002 **4751**

Figure 2. Mulliken population analysis of the (a) *syn* and (b) *anti* conformations of the ozone−fluoroethene and ozone−chloroethene transition states at the CASSCF(10,9)/cc-pVTZ level. Values for the independent reactants are given in parentheses.

electron density on C2 and the prevalence of electrostatic effects cause shortening of the O3−C2 distance below O2−C1. Thus, according to our calculations and despite the larger net stabilization of the fluorethene HOMO, **TSF** becomes stable enough for the rate of ozonolysis of fluoroethene to be approximately equal to that of chloroethene. The experiments even indicate that chlorine substitution decreases the rate to a larger extent than does fluorine substitution.[1] Another consequence of the shorter O3−C2 distance will be shortened and enhanced O3−C2 and O1−O2 bonds in the primary fluorozonide, which gives rise to the preferred rupture of the O1−O3 bond so that the formation of the formylfluoride and Criegee intermediate is what would primarily be expected. In **TSCl**s, both C atoms are negatively charged, and the polarization between them is much weaker, which leads to the possibility of stronger orbital interactions between O2 and C1 that gains additional importance over purely electrostatic interactions. The geometrical consequences are just the opposite of those discussed previously: the O2−C1 distance is now shortened to about the same extent as O3−C2 was in **TSF**. However, as will be seen later, this geometry trend will not be preserved in the primary chlorozonide. In the course of descending into the addition product, the prevalence of the interactions between O3 and C2 will be due to the increasing importance of the anomeric effect and increasing polarization by means of the gradual charge transfer along the reaction path. Consequently, the overall expectations as to which of the two O−O bonds is more likely to rupture further in **POZCl** will be the same as that in **POZF**.

The *anti* conformations of the ozone−haloethene transition states are slightly more stable than their *syn* counterparts. The energy difference is 0.32 kcal mol^{-1} for **TSF**s and 0.23 kcal mol^{-1} for **TSCl**s. This difference is surprising, as one would not expect it merely from considerations concerning the alignment of the ozone and haloethene permanent dipoles. Namely, in the *syn* conformation, this alignment is antiparallel and hence should be more favorable than that of the *anti* conformation (i.e., the *syn* approach of the ozone is the one that should be more favorable). The analyses of the ozone and haloethenes alone, in the geometries that they possess in the transition structures, show that the dipole moment vectors make an angle of 155° in the *syn* but only 47° in the *anti* conformation. Nevertheless, such a large difference in the alignments does not manifest itself in large differences in dipole moments in the case of the complete transition structures. The expectation value of the dipole moment operator for *syn*-**TSF** is 2.04 D, which is somewhat smaller than 2.34 D found for the *anti*. Considerations of the two dipole alignments, however, would be more appropriate for prereaction ozone−haloethene van der Waals complexes and would presumably lead to correct conclusions about stabilization trends if these complexes were to be analogous to the ozone−ethene complex[9] in that no charge transfer has yet occurred. Regarding this stabilization, we believe that *syn* prereaction vdW complexes would be more stable than *anti* complexes, although we were unable to find any such complex at the CASSCF(10,9)/cc-pVTZ level (see Kinetics section). However, it was already mentioned that in all ozone−

haloalkene transition structures the charge transfer from haloalkene to the ozone moiety occurs by leaving the latter negatively charged. Consequently, ozone tries to avoid the negative region of the haloalkenes and favors the *anti* transition-state conformations over the *syn*. Indeed, *anti* conformations have smaller norms of both nuclear (heavy nuclei are more apart) and electronic (the aforementioned reason) contributions to the dipole moment, but in *syn* conformations, these two oppose each other better, hence the smaller total dipole moment.

3. Primary Addition Products. 3a. Primary Ozonide. At the CASSCF(10,9)/cc-pVTZ (Table 1) level of theory, the **POZ** conformation with the lowest energy is an oxygen envelope of C_s symmetry, in agreement with the experimental findings.[8] The calculated geometric parameters are also in a reasonably good agreement with the experiment. The largest deviations are found in the C−O bonds, which are 0.027 Å too long, and the C−C bond, which is 0.018 Å too short. Electronic density in the region of the two C−O bonds is completely included in the **POZ** active space and can be considered to stem dominantly from the ozone LUMO−ethene HOMO and the ozone HOMO−ethene LUMO interactions with respective occupation numbers of 1.9742 and 1.9696. Hence, a considerably better agreement with the experiment in this respect cannot be expected by enlarging the active space or basis set but only by utilizing multireference-based correlated methods. The σ bond between C atoms is too low in energy and is therefore absent from the (10,9) active space.

The lowest vibrational wavenumber (147 cm^{-1}) corresponds to the pseudorotational ring-twisting mode and can be compared to the spectral assignment of 98 cm^{-1}. This movement leads to the half-chair conformation of C_2 symmetry whereby the ring undergoes an inversion without ever becoming planar. The half-chair calculated at the CASPT2(10,9)/cc-pVTZ level is a saddle-point 5.2 kcal mol^{-1} (1810 cm^{-1}) above the oxygen envelope, in good agreement with some other theoretical findings.[10b,32] The second lowest wavenumber (437 cm^{-1}), which is believed to be above 200 cm^{-1} according to ref 8, corresponds to the ring-bending mode and inverts the oxygen envelope by passing through the planar conformation of C_{2v} symmetry, actually a saddle point of order 2. Along the first transition vector, the envelope is inverted, and along the second, the half-chair conformation is formed. The planar conformation suffers too high a ring strain, as can be seen by inspection of the bond lengths (for instance, d(O−O) = 1.473 Å). For this reason, it is somewhat higher in energy, 8.2 kcal mol^{-1} (2870 cm^{-1}), above the oxygen envelope, which compares well to the 2700 cm^{-1} value calculated by Cremer.[10b] Another quantity that can be directly compared to the experiment is the dipole moment. The moment calculated as the expectation of the dipole moment operator is 3.54 D, and the experimentally determined value is 3.43 D.[8] In connection to that value, the Mulliken population analysis shows that the apical oxygen is 0.12*e* less negative than the oxygens bonded to the carbons, which is contrary to the conclusion from the dipole components analysis in ref 8.

3b. Primary Fluorozonide and Chlorozonide. We found two conformational minima of the primary fluoro- and chlorozonide (**POZF** and **POZCl**): one (*syn*) results from descent along the reaction path starting from the *syn*-**TS**, and the other (*anti*), starting from the *anti*-**TS**. It should be noted here that the *syn* and *anti* labels are retained only in connection to the "parent" transition states and are not meant to reflect the actual properties of the X−C2−O3−O1 dihedrals, as these are now somewhat changed (Tables 3 and 4).

The optimizations were carried out with the aim of preserving the same active spaces as those in the transition states, which
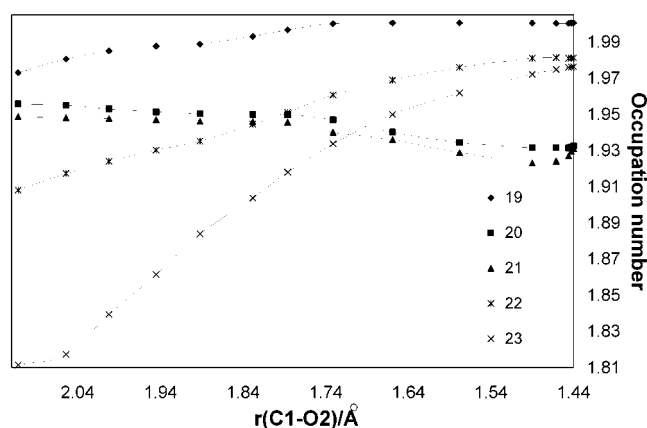

Figure 3. Active orbital (19−23) occupation number dependency upon the C1−O2 distance (Å) in the course of the optimization of *syn*-fluorozonide at the CASSCF(10,9)/cc-pVTZ level.

finally enabled us to establish a clear one-to-one correspondence between the active orbitals of transition states and primary addition products. For this reason, the initial geometries for optimization were constructed by only slightly distorting the transition structures toward products, and the corresponding TS density matrices were taken as the starting points. By utilizing such similar geometries, we completely avoided large initial rotations in the active orbitals and their consequently large modifications and thus managed to preserve the same overall structure of the wave functions. The price to pay was, of course, the many iterations required to reach the optimized product geometries. Nevertheless, such a procedure has an advantage in that an analysis of the "destiny" of all orbitals (i.e., their role in the gradual forming of the bonds) is made possible by following the changes in the occupation numbers throughout the many iteration optimizations such as those along an approximate minimum energy path (Figures 3 and 4). The orbitals are labeled from 19 to 23 in descending order of occupation numbers as they are in the transition states (Figure 5).

Two courses of optimization are given, one for *syn*-**TSF** descending into *syn*-**POZF** and the other for the corresponding pair of *anti* structures. The C1−O2 distance is given as an approximate reaction coordinate and is enough to describe the whole *syn* and the first stage of the *anti* optimization. The second stage of the *anti* optimization is found to be best described by the changes in the δ(H1−C1−C2−F) dihedral angle. Completely analogous trends were observed during the **POZF** and **POZCl** optimizations. The resulting one-to-one correspondence between orbitals in the transition states and **POZF**s can easily be established, as shown in the orbital correlation diagram for the fluoroethene ozonolysis (Figure 5).

Thus, throughout the optimization, the orbital with the largest occupation number in all transition states (19), once responsible for the partial double character of the bonds in ozone, quickly becomes nonbonding and occupies the region of the lone pairs on O atoms. Judging from its high occupation number, already around 1.9 Å for the C1−O2 distance, the orbital completely lost its significance in describing the near-degeneracy effects. Consequently, the four remaining bonding ("occupied") active orbitals are from this point on almost exactly complemented by their antibonding ("virtual") partners, with the sum of each pair of occupation numbers being 2.00. A measure of the bond order can be calculated as the difference between the bonding and corresponding antibonding occupation divided by 2.[16] Two almost equally important bonding interactions of the σ type stem from the dominant contributions of the ozone LUMO−(halo)-
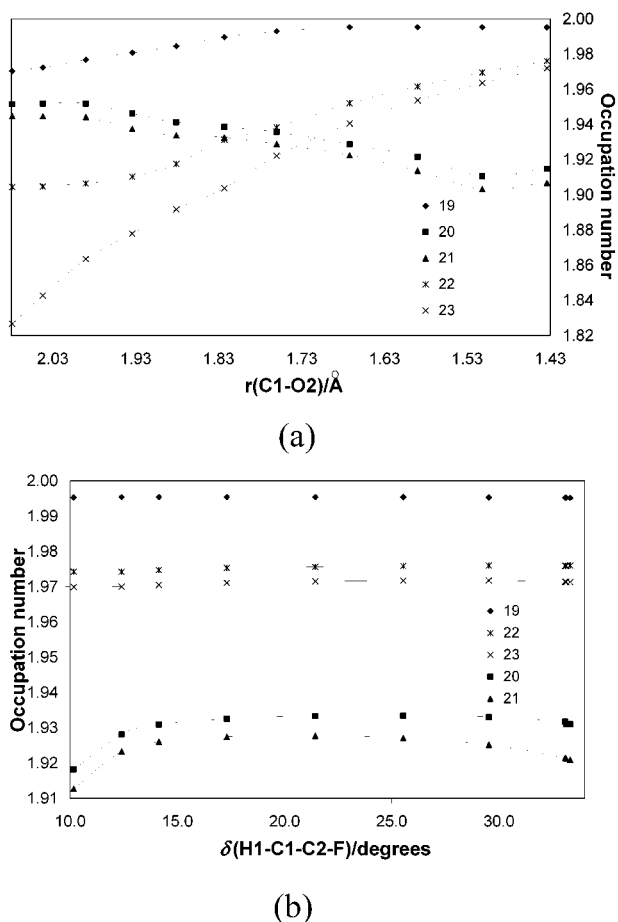
(a)

(b)

Figure 4. Active orbital occupation number (19−23) dependency upon (a) the C1−O2 distance (Å) and (b) the H1−C1−C2−F dihedral angle (deg) in the course of the optimization of *anti*-fluorozonide at the CASSCF(10,9)/cc-pVTZ level.

Figure 5. Orbital correlation diagram and occupation numbers at the CASSCF(10,9)/cc-pVTZ level for the *syn* and *anti* ozonolyses of fluoroethene. The whole active space of fluoroethene and a part of the spaces of ozone, the transition state, and the primary addition product are shown. Beneath each orbital, its occupation number is given as *syn(anti)*.

alkene HOMO (22) and the ozone HOMO−(halo)alkene LUMO (23). Their respective bond orders for **TSF**s are 0.91(0.91) and 0.77(0.79) for *syn(anti)* and 0.98 and 0.97 in **POZF**s, equal for *syn* and *anti*. The former stronger interaction is typical for the C2−O3 pair in **TSF**s and for the C1−O2 pair in **TSCl**s. The forming of the bonds happens in nearly the same uniform monotonic manner and ends near the 1.5 Å C1−O2 distance, with a shallow minimum. Unlike in the transition states, the orbitals describing an interaction between the apical O and the O3 and O2 atoms (20 and 21) gain an increased importance for the near-degeneracy effects, and in the final product, their occupations are less than that of orbitals describing the C−O interactions. This switch happens nearly in the 1.80−1.65 Å region and is a reflection of the charge transfer from haloalkenes to ozone along the reaction path. The transfer gradually causes both O−O bonds to become less polarized, whereas the polarization in the C−O bonds simultaneously increases. In the aforementioned region, the O−O bonds finally become weaker than the C−O bonds. The final O−O bond orders are 0.93-(0.93) and 0.93(0.92). The difference in lengths and therefore in strengths of the final O−O bonds is best depicted in the (HOMOs-1) where a shift of the electron density from the O1−O3 region to the O1−O2 region can be observed in each haloozonide. The countereffect always observed in the HOMOs seems inadequate to completely compensate for this loss. In the second stage of the *anti* optimization, which pertains to the changes in the H1−C1−C2−F dihedral angle, the occupations of the C−O bonds are only mildly increased, which reflects their strengthening due to the increasing anomeric effect (see
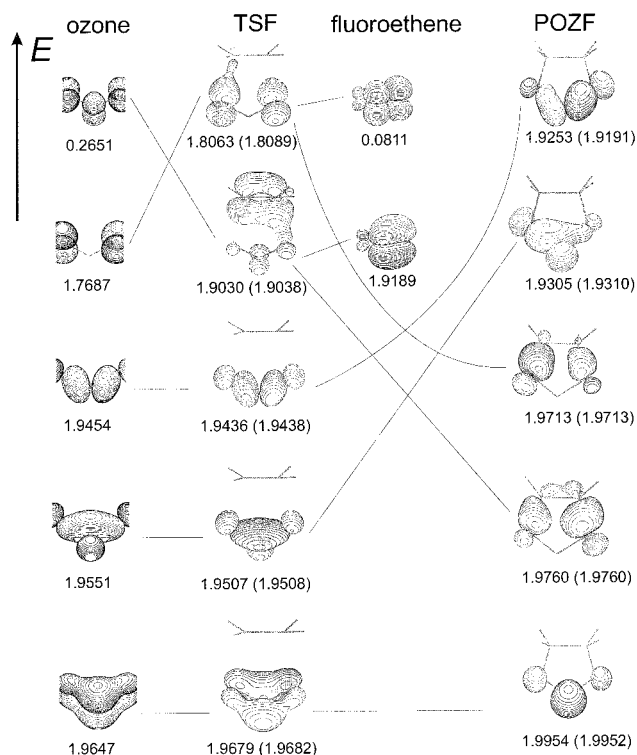
below). At first, the effect seems to stabilize the O−O bonds as well, but their weakening at the end, as revealed by the gradual diminishing of their occupations, is presumably a consequence of simultaneous enlarging of the ring strain.

Very similar geometrical trends are observed for the two pairs of *syn*- and *anti*-**POZF** and **POZCl** conformations. However, unlike the situation in the **TS**s, the *syn* conformations are more stable in both cases. The stability gain of the *syn* conformations over the *anti* is 2.3 kcal mol⁻¹ for **POZF** and 1.7 kcal mol⁻¹ for **POZCl**. As mentioned previously, the geometry trend from **TSCl**s characterized by the shorter C1−O2 distance is not preserved in **POZCl**s. Thus, analogously to that for the **POZF**, the shortening and enhancing of the C2−O3 bond in **POZCl** indicates a preferred cleavage to a formylchloride and a Criegee intermediate. The *syn* conformations, especially *syn*-**POZF**, are characterized by a pronounced eclipsing of the vicinal pairs of H atoms as well as of H and halogen atoms, the dihedral angles δ(H2−C1−C2−H3) and δ(H1−C1−C2-X) equaling −0.2°-(6.4°) and 2.3°(10.8°) for **POZF**(**POZCl**). Unlike them, the *anti* conformations are significantly staggered, (δ(H2−C1−C2−H3) = 36.5°(33.0°) and δ(H1−C1−C2− X) = 33.0°(28.3°)). Their overall method of distortion closely resembles that of the transition-state structure, labeled **TSX**ₒₒₙf, for the inversion and interchange between the two conformations. It was seen in the case of **POZ** how the oxygen envelope of the trioxolane ring represents its most stable conformation. If it does not persist, however, there must be a good reason. An electronegative atom, such as fluorine or chlorine, bonded to a carbon that is adjacent to another atom possessing lone electron pairs results in the well-known and well-understood anomeric effect.[33] The distortion trends of the *anti* conformations can be explained in terms of the anomeric effect, which involves the lone pairs on the O3 atom and the C2 halogen bond. The two must have a near-
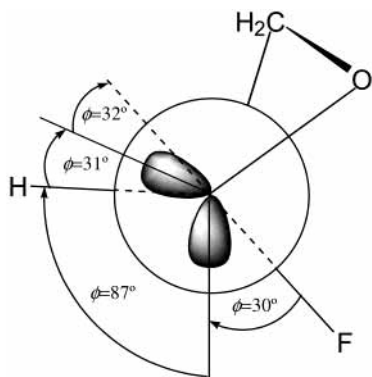
Figure 6. Newman representation along the C2−O3 bond in the analysis of the anomeric effect in fluoroethene.
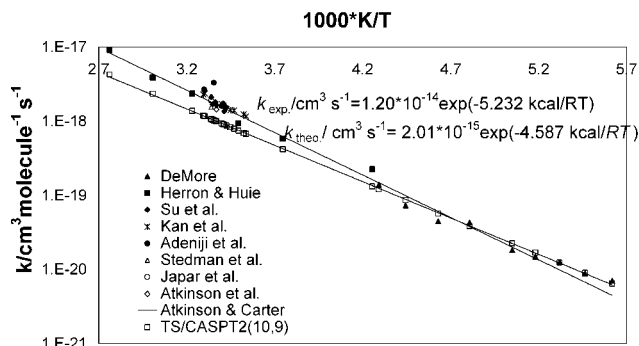

Figure 7. Experimental data and the Arrhenius plot calculated at the CASPT2(10,9)/cc-pVTZ level for the ozonolysis of ethene.
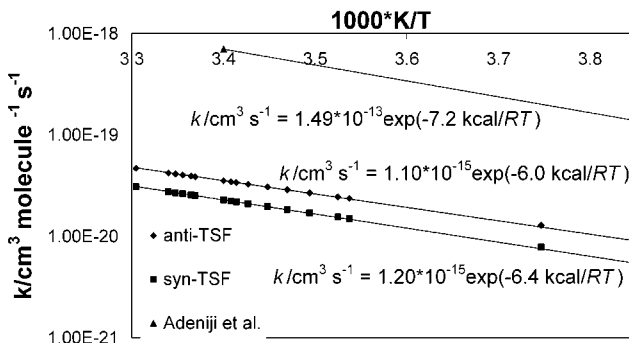

Figure 8. Experimental data and the Arrhenius plot calculated at the CASPT2(10,9)/cc-pVTZ level for the ozonolysis of fluoroethene.
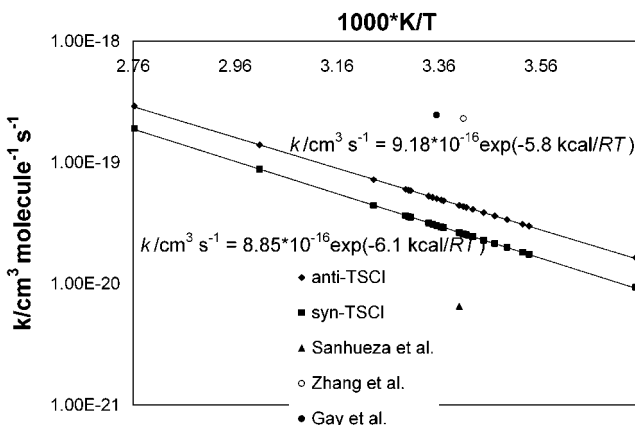

Figure 9. Experimental data and the Arrhenius plot calculated at the CASPT2(10,9)/cc-pVTZ level for the ozonolysis of chloroethene.

parallel mutual alignment to maximize this type of stabilization (the corresponding dihedral equaling 0° or 180°). However, as the ring strain is simultaneously enlarged, as revealed by a substantial prolonging of the O1−O3 bond, the final geometry of the *anti*-halozonides reflects a balance between the two effects, one stabilizing and the other destabilizing. In the *syn* conformations, on the other hand, qualitative analysis of the orientation of the lone pairs with regard to the C−halogen bond revealed that the alignment is already favorable enough with the oxygen envelope retained. In this analysis, the C2−O3 and O1−O3 bonds in *syn*-fluorozonide were observed as approximate edges of a tetrahedron (the deviation in the C2−O3−O1 angle from the tetrahedral is only 7°), and the O3 lone pairs were taken as stretching along the remaining two edges. Then the analytically derived orientation of the O3 lone pairs proved that the alignment of both these pairs is already favorable enough with the C2−F bond but is not so for the C2−H3 bond (Figure 6).

As a consequence, the geometry of the *anti* conformation cannot be simply analogous to the *syn* and be derived from it just by switching the positions of the F and H atoms. An inspection of the active orbital coefficients pertaining to the p functions on the O3 atom and thus determining their spatial orientations completely confirmed these qualitative predictions. As a result and regarding the destabilization due to any deflection from the oxygen envelope, no further distortion can significantly improve the stability of the *syn* conformations so that the oxygen envelope is nearly retained. Besides that, it can be shown that the anomeric alignment is more favorable than that in the *anti* conformations. As another usual consequence of the anomeric effect is shortening of the C2−O3 bond and prolonging of the C2−halogen bond, the same can be concluded by inspection of the C2−O3 bond length, which is shorter for *syn*-**POZF** and *syn*-**POZCl**. The net result is more stable *syn* conformations.

The path to the transition-state structure **TSX**$_{conf}$ starting from the *syn* conformation can be described as a mutual counter-rotation of approximately fixed CH_2O and CHXO moieties. In the meantime, the apical O undergoes a peculiar movement, an asymmetric stretch, whereby the X−C2−O3−O1 dihedral is reduced by about 10°. The consequences are very interesting; the O1−O2 bond is elongated by 0.3 Å but O1−O3, by only 0.1 Å! This occurrence switches their relative strengths for a moment, which can be seen as a shift in electron density in the (HOMOs-1) from one O−O bond region to the other. The described trends are shown to be governed mainly by the anomeric effect and simultaneous mutual repulsion between lone pairs on the O-atoms due to a serious deflection from the oxygen envelope. Finally, it can be concluded that if the Criegee cleavage is to happen near the **TSX**$_{conf}$ region of the PES, then,

unlike before, formaldehyde and halogen Criegee intermediates will primarily result.

B. Reaction Kinetics

The experimental and calculated Arrhenius plots for the ozonolyses of ethene, fluoro-, and chloroethene are shown in Figures 7, 8, and 9, respectively, and the corresponding potential-energy diagrams, in Figures 10, 11, and 12. The reaction rates are calculated in terms of the conventional transition-state theory according to the equation

$$k(T) = \left(\frac{k_B T}{h}\right) \frac{Q^{\ddagger}}{Q_r} \exp[-\Delta E_0^{\ddagger}/RT]$$

where the Q's are the partition functions of the activated complex ($\ddagger$) and the reactants (r), and $\Delta E_0^{\ddagger}$ is the height of the reaction barrier corrected for the differences in ZPEs.

Figure 10. One-dimensional potential-energy diagram for the ozonolysis of ethene calculated at the CASPT2(10,9)/cc-pVTZ level. All electronic energies are corrected for the zero-point vibrational energies.
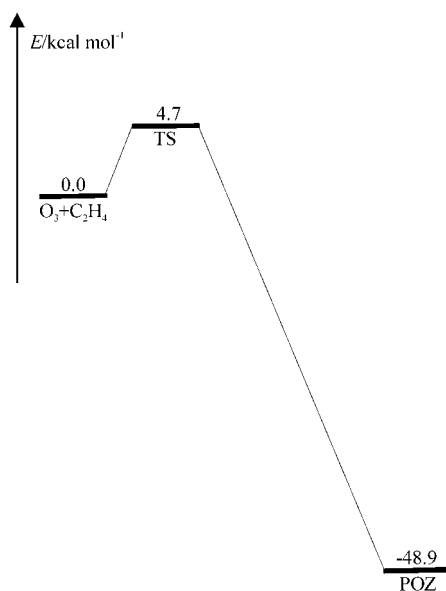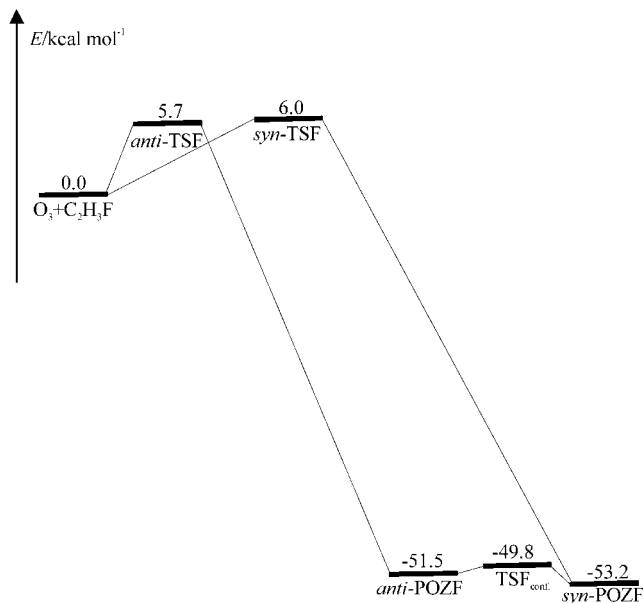

Figure 11. One-dimensional potential-energy diagram for the ozonolysis of fluoroethene calculated at the CASPT2(10,9)/cc-pVTZ level. All electronic energies are corrected for the zero-point vibrational energies.

A great abundance of experimental work was done on ethene, and we report the most reliable and reproducible results characterized by a relatively small amount of scatter. Although our calculated reaction barrier is 0.6 kcal mol^{-1} smaller than the experimental value, the overall rate values for the plotted temperature range are closer than what is expected from this difference. This result is due to the order-of-magnitude flaw in the calculated preexponential factor. Thus, the calculated rate constant at 298 K is 1.02×10^{-18} cm^3 molecule^{-1} s^{-1}, in very good agreement with the experimental value.[1] The overall agreement in rates is better for lower temperatures, which are typical for higher altitudes of the troposphere.

The scarcity of experimental data for ozonolyses of fluoroethene and chloroethene diminishes the relevance of comparing the calculated and experimental values. Thus, in case of
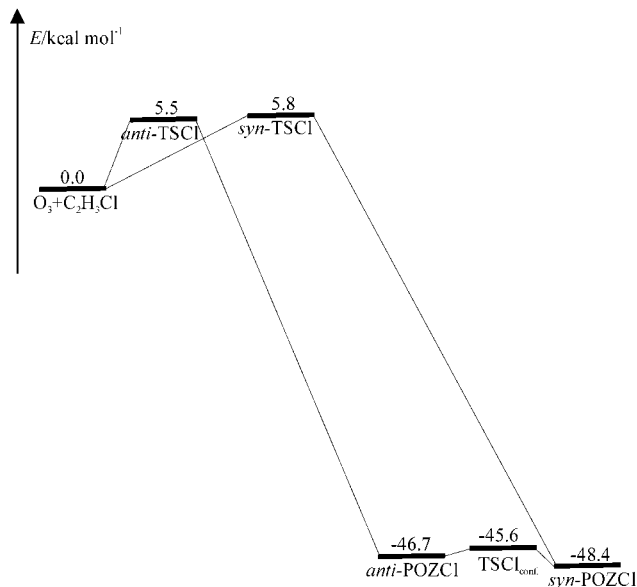

Figure 12. One-dimensional potential-energy diagram for the ozonolysis of chloroethene calculated at the CASPT2(10,9)/cc-pVTZ level. All electronic energies are corrected for the zero-point vibrational energies.

fluoroethene, the Arrhenius parameters were derived from only two experimental points, and the experimental value was found to be 78.1×10^{-20} cm^3 molecule^{-1} s^{-1} at 298 K. The calculated rate constants are 4.03×10^{-20} cm^3 molecule^{-1} s^{-1} for the *anti* and 2.62×10^{-20} cm^3 molecule^{-1} s^{-1} for the *syn* reaction at 298 K. The three available data points for chloroethene display such large scatter that no recommendation of the reaction rate and Arrhenius parameters is possible.[1] The plot based on our calculated values passes somewhere through the "middle" of the experimental scatter, and the rate constant at 298 K is 5.03×10^{-20} cm^3 molecule^{-1} s^{-1} for *anti* and 3.02×10^{-20} cm^3 molecule^{-1} s^{-1} for *syn* reaction energies. Thus, according to our calculations, the ozonolysis of chlororethene should be only slightly faster than that of fluoroethene.

The reaction enthalpy 48.9 kcal mol^{-1} for the ethene ozonolysis is in good agreement with some recent theoretical estimates and the experimental value[7] of 45 ± 6 kcal mol^{-1}. The latest theoretical result at the CASSCF(10,9)/6-31G(d) level[6] predicts 49.2 kcal mol^{-1}, and the other estimates[3b,f,5] range from 43.7 to 57.3 kcal mol^{-1}. As to the haloalkenes' ozonolyses, the exothermicity order in the reaction enthalpies is in agreement with some earlier predictions concerning influences of the halogen substituent on the trioxolane ring.[3e] Although the absolute reaction enthalpies for the ozonolyses of ethene and fluoroethene at the RHF/6-31G* level[3c,e] are far too high, their relative difference of -5.1 kcal mol^{-1} is still acceptable compared to ours of -4.3 kcal mol^{-1}. From the three calculated thermally corrected (298 K) enthalpies of the ozonolyses and the experimental gaseous enthalpies of formation of ozone (34.1 kcal mol^{-1}), ethene (12.5 kcal mol^{-1}), fluoroethene (-32.5 kcal mol^{-1}), and chloroethene (6.9 kcal mol^{-1})[34] at 298 K, the standard enthalpies of formation of ozonide, fluorozonide, and chlorozonide at 298 K are calculated to be -2.9 kcal mol^{-1}, -51.9 kcal mol^{-1}, and -8.1 kcal mol^{-1}, respectively. To bring these three enthalpies onto approximately the same footing, one-half of the difference between the H−H bond strength (104.2 kcal mol^{-1})[34] and the F−F (37.5 kcal mol^{-1}) and Cl−Cl (58.0 kcal mol^{-1}) bond strengths, respectively, for **POZF** and **POZCl** were added to the respective enthalpies. As a result, the fluorine substitution stabilizes the trioxolane ring by about 16 kcal mol^{-1},

4756 *J. Phys. Chem. A, Vol. 106, No. 18, 2002*

Ljubić and Sabljić

which is comparable to the 12 kcal mol^{-1} value given by Cremer.[3e] However, chlorine substitution destabilizes the ring by about 18 kcal mol^{-1}, which should make the primary chlorozonide very difficult to isolate.

It must be noted that prereaction van der Waals complexes are likely to exist for ozonolyses of the haloethenes analogous to that between ozone and ethene, which was successfully isolated and analyzed.[9] However, the theoretical approach used in the present study does not allow us to draw definite conclusions as to their existence. Their effect on the kinetics would be in raising all the barriers, and thus the calculated values would more closely approach the experimental ones. Considering the type of interaction, which is either dipole−dipole or dipole−induced dipole, the amount of stabilization is presumably fluoroethene > chloroethene > ethene. Nevertheless, we were not able to find any reasonable structure for the supposed ozone−haloethene prereaction complexes. It is known that the necessary conditions for a reliable description of weak complexes include at least the use of TZ+P basis sets and especially a method that largely covers the effects of dynamic correlation.[35] However, the absence of the complexes from our PESs is presumably not only due to the inefficient amount of dynamic correlation comprised by the CASSCF method but also due to the expected very shallow minima. Thus, an approximate structure of the ozone−ethene complex was obtained at the CASSCF(10,9)/cc-pVTZ level by adopting the Baker convergence criteria[36] and by significantly reducing the value that defines the largest change in the internal coordinates during optimization. Unfortunately, here the CASPT2 and CASSCF stationary geometries do not coincide well, and consequently the CASSCF geometry does not have the necessary stabilization at the CASPT2 level, as it is not close enough to what would be the CASPT2 minimum. Another problem is posed by the basis set superposition error (BSSE) estimate because no prescription exists of how the counterpoise (CP) correction[37] should be best applied if multireference methods are used. Namely, it is not clear what the active space size of the two fragments should be in the ghost basis of their partners. Without the CP correction, the stabilization of 0.51 kcal mol^{-1} was obtained for the prereaction vdW complex of ozone and ethene at the CASSCF(10,9)/cc-pVTZ level. Applying the CP correction with the (8,7) active space on ozone and the (2,2) active space on ethene in the ghost basis of each other reduced the value to 0.24 kcal mol^{-1}. The latter value is not in a good agreement with 0.74 kcal mol^{-1} obtained at the MP4(SDTQ)/6-31G(d,p) level.[9]

Conclusions

In this work, we utilized the multiconfiguration CASSCF and multireference CASPT2 methods with a large basis set and active spaces for investigating the formation of the primary addition products in ozonolyses of ethene, fluoroethene, and chloroethene. This work was performed by a thorough geometrical and electronic structure analysis of the two basic trends of ozone approach in the case of the two haloalkenes and the resulting two conformations of the primary addition products. Moreover, it was shown that valuable and complementary information is possible to obtain by analyzing the trends in the occupations of active orbitals in the course of the reactions. Indeed, it can be said that such a procedure, in an otherwise static analysis, returned some of the necessary dynamics to each of the processes observed. It was seen how a relatively cheap method of energy refinement as CASPT2 in combination with CASSCF optimized geometries gives very good results for the kinetics of ozonolysis of the three simple alkenes. Moreover, these results are quite comparable to incomparably more expensive and elaborate post-HF treatments. Whereas CASPT2 corrections can be obtained in a reasonably short amount of time after the optimizations, a single-point CCSD(T)/cc-pVTZ calculation, for instance, on any of the systems of interest turned out to be prohibitively large for our computational resources. The two calculated reaction barriers of ozonolysis are within the limits of chemical accuracy ($\sim\pm1$ kcal mol^{-1}) when compared to the experimental reaction studies of ethene and the one available study for fluoroethene. The lack of coherent and reliable experimental data for chloroethene prevents us from drawing a similar conclusion for this case. However, our calculated values lie somewhere between the scattered experimental points, so we believe that the methods utilized in this work are reasonably reliable in the case of the ozonolysis of chloroethene as well. The two basic ways of ozone approach to the haloalkenes were considered, and the obtained trends in stationary energies differ for the transition states and the final addition products. While the *syn* conformations of TSs are slightly destabilized as compared to those of the *anti*, the *syn* products are considerably more stabilized. We conclude that the trends in energy are at first governed by the electrostatic repulsion and later by the anomeric effect. The latter effect also plays an important role in the course of the interchange between the two primary addition product conformations. Although ozone−haloalkene vdW complexes are likely to exist prior to the transition states, none of them was found for either conformation at the CASSCF(10,9)/cc-pVTZ level. Considering the strengths and types of interactions, an increasingly sophisticated correlated method would presumably show the stabilization in the *syn* complexes to be larger than that in the *anti* (more favorable alignment of the permanent dipole moments) and the fluoroethene complex to be more stabilized than the corresponding chloroethene complexes (stronger dipole−dipole interactions). Both are expected to be more stable than the prereaction ozone−ethene vdW complex. Further work aimed at shedding more light on the subsequent steps of the ozonolyses of the two haloalkenes is currently in progress.

Supporting Information Available: Cartesian coordinates (bohr) and CASSCF and CASPT2 energies (hartree) for all stationary points discussed in the paper. This material is available free of charge via the Internet at http://pubs.acs.org.

References and Notes

(1) Atkinson, R.; Carter, W. P. L. *Chem. Rev.* **1984**, *84*, 437.

(2) Bailey, P. S. *Ozonization in Organic Chemistry*; Academic Press: New York, 1978; Vol. 1.

(3) (a) Harding, L. B.; Goddard, W. A., III. *J. Am. Chem. Soc.* **1978**, *100*, 7180. (b) Cremer, D. *J. Chem. Phys.* **1979**, *70*, 1898. (c) Cremer, D. *J. Am. Chem. Soc.* **1981**, *103*, 3619. (d) Cremer, D. *J. Am. Chem. Soc.* **1981**, *103*, 3627. (e) Cremer, D. *J. Am. Chem. Soc.* **1981**, *103*, 3633. (f) Dewar, M. J. S.; Hwang, J. C.; Kuhn, D. R. *J. Am. Chem. Soc.* **1991**, *113*, 735. (g) Cremer, D.; Kraka, E.; McKee, M. L.; Radhakrishnan, T. P. *Chem. Phys. Lett.* **1991**, *187*, 491. (h) Cremer, D.; Gauss, J.; Kraka, E.; Stanton, J. F.; Bartlett, R. *Chem. Phys. Lett.* **1993**, *209*, 547. (i) Ponec, R.; Yuzhakov, G.; Haas, Y.; Samuni, U. *J. Org. Chem.* **1997**, *62*, 2757.

(4) Fenske, J. D.; Hasson, A. S.; Paulson, S. E.; Kuwata, K. T.; Ho, A.; Houk, K. N. *J. Phys. Chem. A* **2000**, *104*, 7821 and references therein.

Ozonolyses of Ethene and Fluoro- and Chloroethene

J. Phys. Chem. A, Vol. 106, No. 18, 2002 **4757**

(5) Olzmann, M.; Kraka, E.; Cremer, D.; Gutbrod, R.; Andersson, S. *J. Phys. Chem. A* **1997**, *101*, 9421.

(6) Anglada, J. M.; Crehuet, R.; Bofill, J. M. *Chem.—Eur. J.* **1999**, *5*, 1809.

(7) Nangia, P. S.; Benson, S. W. *J. Am. Chem. Soc.* **1980**, *102*, 3105.

(8) Gillies, J. Z.; Gillies, C. W.; Suenram, R. D.; Lovas, F. J. *J. Am. Chem. Soc.* **1988**, *110*, 7991.

(9) Gillies, C. W.; Gillies, J. Z.; Suenram, R. D.; Lovas, F. J.; Kraka, E.; Cremer, D. *J. Am. Chem. Soc.* **1991**, *113*, 2412.

(10) (a) Criegee, R. *Rec. Chem. Proc.* **1957**, *18*, 111. (b) Criegee, R. *Angew. Chem.* **1975**, *87*, 765.

(11) Dowideit, P.; von Sonntag, C. *Environ. Sci. Technol.* **1998**, *32*, 1112.

(12) Roos, B. O. In *Lecture Notes in Quantum Chemistry*; Roos, B. O., Ed.; Springer-Verlag: Berlin, 1992; pp 177–255.

(13) (a) Lee, T. J. *J. Chem. Phys.* **1990**, *93*, 489. (b) Lee, T. J. *Chem. Phys. Lett.* **1990**, *169*, 529. (c) Leininger, M. L.; Schaefer, H. F. *J. Chem. Phys.* **1997**, *107*, 9059. (d) Watts, J. D.; Bartlett, R. J. *J. Chem. Phys.* **1998**, *108*, 2511.

(14) (a) Xantheas, S. S.; Atchity, G. J.; Elbert, S. T.; Ruedenberg, K. *J. Chem. Phys.* **1991**, *94*, 8054. (b) Borowski, P.; Andersson, K.; Malmqvist, P.-Å; Roos, B. O. *J. Chem. Phys.* **1992**, *97*, 5568. (c) Tsuneda, T.; Nakano, H.; Hirao, K. *J. Chem. Phys.* **1995**, *103*, 6520. (d) Li, X.; Paldus, J. *J. Chem. Phys.* **1999**, *110*, 2844.

(15) (a) Roos, B. O.; Taylor, P. R.; Siegbahn, P. E. M. **1980**, *48*, 157. (b) Andersson, K.; Malmqvist, P.-Å.; Roos, B. O. *J. Chem. Phys.* **1992**, *96*, 1218. (c) Andersson, K.; Malmqvist, P.-Å.; Roos, B. O.; Sadlej, A. J.; Wolinski, K. *J. Phys. Chem.* **1990**, *94*, 5483.

(16) Roos, B. O. In *European Summerschool in Quantum Chemistry*, book II; Roos, B. O., Widmark, P. O., Ed.; Lund University, 2000; pp 349–357.

(17) (a) Pelzer, H.; Wigner, E. *Z. Phys. Chem., Abt. B* **1932**, *15*, 445. (b) Eyring, H. *J. Chem. Phys.* **1935**, *3*, 107. (c) Glasstone, S.; Laidler, K.; Eyring, H. *The Theory of Rate Processes*; McGraw-Hill: New York, 1941.

(18) Anglada, J. M.; Bofill, J. M. *Chem. Phys. Lett.* **1995**, *243*, 151.

(19) (a) Dunning, T. H., Jr. *J. Chem. Phys.* **1989**, *90*, 1007. (b) Woon, D. E.; Dunning, T. H., Jr. *J. Chem. Phys.* **1993**, *98*, 1358.

(20) Andersson, K.; Blomberg, M. R. A.; Fülscher, M. P.; Karlström, G.; Lindh, R.; Malmqvist, P.-Å.; Neogrády, P.; Olsen, J.; Roos, B. O.; Sadlej, A. J.; Schütz, M.; Seijo, L.; Serrano-Andres, L.; Siegbahn, P. E. M.; Widmark, P.-O. *MOLCAS*, version 4.1; Lund University: Sweden 1997.

(21) Andersson, K.; Barysz, M.; Berndhardsson, A.; Blomberg, M. R. A.; Cooper, D. L.; Fleig, T.; Fülscher, M. P.; de Graaf, C.; Hess, B. A.; Karlström, G.; Lindh, R.; Malmqvist, P.-Å.; Neogrády, P.; Olsen, J.; Roos, B. O.; Sadlej, A. J.; Schütz, M.; Schimmelpfennig, B.; Seijo, L.; Serrano-Andres, L.; Siegbahn, P. E. M.; Stårling, J.; Thorsteinsson, T.; Veryazov, V.; Widmark, P.-O. *MOLCAS,* version 5; Lund University: Sweden, 2000.

(22) Corchado, J. C.; Chuang, Y.-Y.; Fast, P. L.; Villa, J.; Coitino, E. L.; Hu, W.-P.; Liu, Y.-P.; Lynch, G. C.; Nguyen, K.; Jackels, C. F.; Gu, M. Z.; Rossi, I.; Clayton, S.; Melissas, V.; Steckler, R.; Garrett, B. C.; Isaacson, A. D.; Truhlar, D. G. *POLYRATE*, version 7.8; copyright 1988-1997, Truhlar, D. G., Regents of the University of Minnesota.

(23) (a) DeMore, W. B. *Int. J. Chem. Kinet.* **1969**, *1*, 209. (b) Stedman, D. H.; Wu, C. H.; Niki, H. *J. Phys. Chem.* **1973**, *77*, 2511. (c) Herron, J. T.; Huie, R. E. *J. Phys. Chem.* **1974**, *78*, 2085. (d) Japar, S. M.; Wu, C. H.; Niki, H. *J. Phys. Chem.* **1974**, *78*, 2318. (e) Japar, S. M.; Wu, C. H.; Niki, H. *J. Phys. Chem.* **1976**, *80*, 2057. (f) Toby, F. S.; Toby, S.; O'Neal, H. E. *Int. J. Chem. Kinet.* **1976**, *8*, 25. (g) Su, F.; Calvert, J. G.; Shaw, J. H. *J. Phys. Chem.* **1980**, *84*, 239. (h) Adeniji, S. A.; Kerr, J. A.; Williams, M. R. *Int. J. Chem. Kinet.* **1981**, *13*, 209. (i) Atkinson, R.; Aschmann, S. M.; Fitz, D. R.; Winer, A. M.; Pitts, J. N., Jr. *Int. J. Chem. Kinet.* **1981**, *14*, 13. (j) Kan, C. S.; Su, F.; Calvert, J. G.; Shaw, J. H. *J. Phys. Chem.* **1981**, *85*, 2359.

(24) (a) Sanhueza, E.; Hisatsune, I. C.; Heicklen, J. *Chem. Rev.* **1976**, *76*, 801. (b) Gay, B. W., Jr.; Hanst, P. L.; Bufalini, J. J.; Noonan, R. C. *Environ. Sci. Technol.* **1976**, *10*, 58. (c) Zhang, J.; Hatakeyama, S.; Akimoto, H. *Int. J. Chem. Kinet.* **1983**, *15*, 655.

(25) Harmony, M. D.; Laurie, V. W.; Kuczkowski, R. L.; Schwendeman, R. H.; Ramsay, D. A.; Lovas, F. J.; Lafferty, W. J.; Maki, A. G. *J. Phys. Chem. Ref. Data* **1979**, *8*, 619.

(26) Sekušak, S.; Liedl, K. R.; Sabljić, A. *J. Phys. Chem. A* **1998**, *102*, 1583.

(27) (a) Herzberg, G. *Molecular Spectra and Molecular Structure. II. Infrared and Raman Spectra of Polyatomic Molecules*; D. van Nostrand Company Inc.: Toronto, 1968. (b) Bak, B.; Christensen, D. *Spectrochim. Acta* **1958**, *12*, 355. (c) Gullikson, C. W.; Rud Nielsen, J. *J. Mol. Spectrosc.* **1957**, *1*, 158.

(28) Güsten, H.; Klasinc, L.; Marić, D. *J. Atmos. Chem.* **1984**, *2*, 83.

(29) Shimanouchi, T. *J. Phys. Chem. Ref. Data* **1977**, *6*, 993.

(30) Ljubić, I.; Sabljić, A., to be submitted for publication.

(31) Tanaka, T.; Morino, Y. *J. Mol. Spectrosc.* **1970**, *33*, 538.

(32) Cremer, D.; Pople, J. A. *J. Am. Chem. Soc.* **1975**, *97*, 1358.

(33) Schleyer, P. v. R.; Kos, A. J. *Tetrahedron* **1983**, *39*, 1141 and references therein.

(34) *CRC Handbook of Chemistry and Physics*, 73rd ed.; Lide, D. R., Ed.; CRC Press: Boca Raton, FL, 1992-1993.

(35) Chałasiński, G.; Szczęśniak, M. M. *Chem. Rev.* **1994**, *94*, 1723.

(36) Baker, J. *J. Comput. Chem.* **1993**, *14*, 1085.

(37) Boys, S. F.; Bernardi, F. *Mol. Phys.* **1970**, *19*, 553.